RESEARCH ARTICLE OPEN ACCESS

Flood Disaster Risk Assessment of the Alluvial-Diluvial Plain in the Piedmont of the Taihang Mountains Based on AHP-CRITIC Combined Weighting

Yixin Pang [1],Haijun Li[1,2,*], Ziyan Zhang[3],Yao Fan [4], Bingbin Du [1] , Shuiqing Zhou [1],Jiachen Lu[1], Xiaoqing Yu[1]
[1] *Institute of Disaster Prevention, Beijing, China Institute of Disaster Prevention, Beijing, China*
[2] *Hebei Key Laboratory of Resource and Environmental Disaster Mechanism and Risk Monitoring, Sanhe, China*
[3] *Rizhao Donggang District Emergency Management Bureau, Rizhao 276800，China*
[4] *Shuifa Planning & Design Co.,Ltd., Jinan 250100,China*

* Correspondence:
Haijun Li
lhjun777@cidp.edu.cn
E-mail addresses: lhjun777@cidp.edu.cn (Haijun Li),24661704@st.cidp.edu.cn (Yixin Pang), zhangziyan0117@163.com (Ziyan Zhang), fanyao2004@126.com (Yao Fan),25661710@st.cidp.edu.cn (Bingbin Du),zhouzhoushuiqing@163.com (Shuiqing Zhou).

--************************----------------------------------

Abstract:

Disaster risk assessment is a crucial component in scientifically formulating disaster prevention and mitigation strategies and achieving effective disaster risk management. Taking the piedmont alluvial plain area of the Taihang Mountains as a case study, this research employs a hazard-exposure-vulnerability-resilience (H-E-V-R) assessment framework. By integrating subjective weights with objective weights derived from the CRITIC method through a game-theoretic combined weighting approach, we quantify the contribution of each factor to flood risk and clarify its spatial distribution characteristics. Results show that flood risk exhibits a distinct spatial pattern—high in the north, central, and southern regions, and low around the periphery. High-risk zones are primarily distributed along major river systems such as the Yongding River, Hutuo River, and Zhangwei River, forming belt-like extensions concentrated in core urban clusters including Beijing, Tianjin, Langfang, Shijiazhuang, and Xinxiang. Low-risk areas appear as scattered patches, mainly located in the inland central plains away from major river networks. The primary influencing factors are distance to waterways (0.2220), rainfall intensity (0.1370), and peak flood discharge (0.1127). Validation using historical flood frequency and inundation depth indicates that the higher-risk zones identified by the combined weighting method match historical disaster-prone areas at a rate of 70.59%, while high-hazard zones align with actual inundated areas at 73.97%. These findings provide scientific basis for flood prevention and control in the Taihang foothill plain region and offer valuable support for regional disaster risk management and planning.

Keywords — **Flood disaster, risk assessment, AHP-CRITIC, game theory-based combined weighting**

--************************----------------------------------

I. INTRODUCTION

Floods are among the most prevalent natural disasters globally, occurring extensively across regions. In 2021 alone, they accounted for approximately 52% of all catastrophic events worldwide [1]、[2]. The devastating impacts of flood disasters are undeniable [3]. Since 2000, China has recorded the highest number of natural disaster events globally, with a total of 577 incidents [4]. From 2001 to 2020, floods in China affected an annual average of over 100 million people, resulting in direct economic losses of 167.86 billion yuan [5]. Major historical flood events, such as the 63·8 heavy rainfall, 96 heavy rainfall, "16·7" heavy rainfall, "21·7" northern Henan heavy rainfall, and "23·7" North China heavy rainfall, have also caused severe casualties and property damage [6]、[7]、[8]、[9].Against the backdrop of global climate change, extreme precipitation events are on the rise, while changes in factors such as surface impermeability and land use further exacerbate flood risks (IPCC, 2021). As a result, the frequency, spatial extent, and potential losses associated with flood disasters are projected to exhibit increasingly complex patterns in the future [10]. Therefore, effectively mitigating flood occurrences has become particularly critical, and flood risk management is a pivotal strategy for reducing both the incidence of floods and their associated damages. Flood risk assessment (FRA) is a core component of flood risk management research. By delineating the spatial distribution of flood risks, FRA can support the formulation of evidence-based flood management policies, rational resource allocation, and the evaluation of flood control measure effectiveness [11]、[12]、[13].

In the field of flood disaster risk assessment, four methods are widely adopted: historical disaster assessment, remote sensing (RS) and geographic information system (GIS) coupling, scenario simulation assessment, and indicator system-based assessment. The historical disaster assessment method extracts regional historical flood risk information and disaster data to characterize the evolutionary patterns of flood disasters. However, its reliance solely on historical disaster records leads to inherent limitations [14]、[15]. The RS-GIS coupling method acquires key hydrometeorological data via remote sensing and evaluates flood risk through visualized data processing, yet it is constrained by the resolution of remote sensing images and the accuracy of image interpretation [15]、[16]、[17]. The scenario simulation assessment method constructs rainfall-flood simulation models and loss assessment models based on GIS and RS to enable dynamic flood risk evaluation, though its effectiveness heavily depends on data precision [15]、[18]、[19]. The indicator system-based assessment method identifies critical indicators from regional influencing factors using predefined criteria, constructs a flood risk assessment framework, and calculates indicator weights to conduct risk evaluation [15]、[19]. This method is suitable for risk research across different scales and can intuitively reflect the correlation between indicators and flood risk [20]、[21].

The indicator system primarily consists of two main components: indicator elements and weights. Based on the flood disaster system, current flood risk assessment frameworks mainly include three approaches: hazard-vulnerability (H-V), hazard-exposure-vulnerability (H-E-V), and hazard-exposure-vulnerability-risk reduction capacity (H-E-V-R) frameworks [17]、[22]. Each framework has its own applicability, and different scholars adopt various frameworks depending on their research contexts. Chen et al. developed a flood risk assessment framework for Taiwan at the end of the 21st century based on the H-V framework, using the RCP8.5 scenario and multiple spatial scales [23]. Bin et al. proposed an urban flood risk assessment method capable of capturing the relationships among the three elements—hazard, exposure, and vulnerability [24]. Zhang et al. conducted a flood risk assessment for the Changsha-Zhuzhou-Xiangtan (CZT) urban agglomeration by selecting 17 socioeconomic and natural environmental factors within a comprehensive risk assessment framework that includes hazard, exposure, vulnerability, and resilience [25]. Regarding weight determination, single weighting methods tend to be one-sided, making combined weighting techniques increasingly popular. Common combinations include FAHP with entropy weight, AHP with CRITIC, and game-theoretic integration. Typical combination methods include linear weighting, multiplicative synthesis, game-theoretic integration, and least squares method. Linear weighting is simple and practical but relies on subjective α values; multiplicative synthesis emphasizes consistency between subjectivity and objectivity yet may excessively compress weights of highly divergent indicators; game-theoretic integration is mathematically rigorous and can automatically optimize fusion coefficients; the least squares method allows integration of multiple methods but risks getting trapped in local optima [26]、[27].

The piedmont alluvial plain of the Taihang Mountains is a transitional zone between mountainous areas and coastal alluvial plains. Given the historical complexity of flood events in this region, conducting flood disaster risk assessment in the piedmont area is of critical significance for flood risk management. Based on the correlations among multiple indicator-based influencing factors, this study adopts a rapid and efficient game-theoretic combined weighting method integrating the Analytic Hierarchy Process (AHP) and Criteria Importance Through Intercriteria Correlation (CRITIC) to evaluate flood risk in the Taihang Mountains' piedmont alluvial plain. This approach delineates key priorities for flood prevention and control in the piedmont region, thereby providing scientific support for regional flood risk management, flood control planning, territorial spatial planning, and decision-making related to disaster prevention and mitigation.

II. MATERIALS AND METHODS

A. Study Area

The study area is situated in the central-northern segment of the North China Plain, predominantly encompassing alluvial-proluvial plain regions formed by piedmont rivers of the Taihang Mountains (Fig. 1). Geographically, it spans latitudes 35.00°N to 40.12°N and longitudes 112.93°E to 117.32°E, extending westward from the eastern foothills of the Taihang Mountains, eastward to central Tianjin, northward to southern Beijing, and southward to northern Henan Province. This region constitutes a critical zone for the formation and convergence of flood disasters in North China.

Climatically, the area falls under a temperate monsoon climate, where precipitation coincides with the high-temperature period. The multi-year average rainfall ranges from 290 to 760 mm, with the highest frequency of rainstorms occurring in summer—particularly concentrated in July and August—accompanied by high storm intensity. During the rainy season, influenced by the convergence of the subtropical high and the Inner Mongolia high, coupled with the west-high-east-low topographic gradient, water vapor is obstructed by the Taihang Mountains, facilitating rainfall formation on the windward slopes. The eastern foothills are characterized by high concentrations of population and infrastructure, rendering the area highly prone to flood disasters [6]、[28].

The study area spans four provincial-level administrative regions: Beijing, Tianjin, Hebei, and Henan. Characterized by high population density and advanced urbanization, this region has witnessed reduced permeable urban surfaces, shrinking water storage capacity of rivers and lakes, and altered runoff discharge pathways. These changes have compromised the capacity for rainwater infiltration, storage, and detention, as well as shortened the confluence time, thereby creating favorable conditions for flood generation [29]、[30]. The "23·7" extreme rainstorm event resulted in 3.8886 million affected people (including 978,400 individuals in flood storage and detention areas), 319,700 hectares of damaged crops, and direct economic losses totaling 95.811 billion yuan.

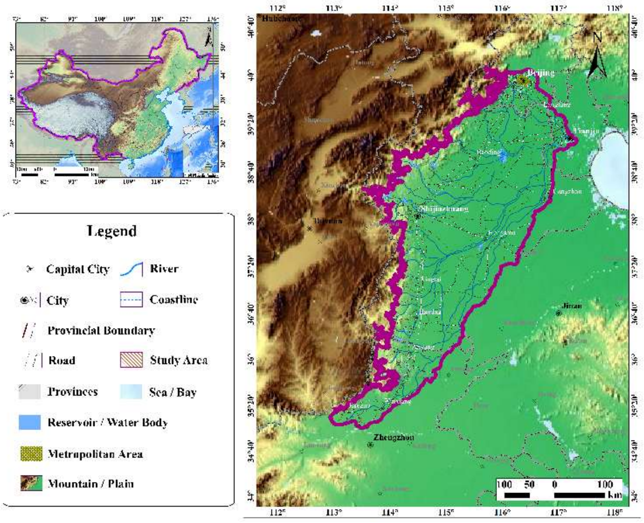

Fig. 1 Overview of the Beijing-Tianjin-Hebei Study Area

B. Research Methodology

1) Construction of the Evaluation Indicator System: Drawing on the historical records of multiple large-scale flood disasters in this region, flood events are not driven by a single influencing factor. Two core factors governing flood formation within the basin are underlying surface parameters and climate change parameters, which are jointly modulated by rainfall, topography, land cover, and other factors [31]. For the comprehensive characterization of flood disaster risk, a holistic assessment extends beyond mere hazard evaluation; the impacts of human activities on flood risks are equally non-negligible. Thus, by integrating the regional context with the conceptual model of disaster risk assessment, twelve critical influencing factors were selected as evaluation indicators, based on four core dimensions: hazard of disaster-causing factors (H), sensitivity of the disaster-predisposing environment (S), vulnerability of disaster-bearing bodies (V), and disaster prevention and mitigation capacity (R). The constructed indicator evaluation system and the data sources of each indicator are presented in Table I.

Continuous intense rainfall acts as a disaster-causing factor, encompassing rainfall amount and duration [32]. In this study, intense rainfall amount, peak flood discharge, and long-term average annual rainfall are selected as evaluation indicators. The long-term average annual rainfall reflects the total annual precipitation and serves as a key metric for assessing the overall annual water supply status of a region. Intense rainfall can elevate river water levels and amplify flood risk—particularly when rivers are unable to convey excess water, intense rainfall may trigger flooding. Peak flood discharge, which represents the maximum volume of water passing through a cross-section during the most severe phase of a flood, is a critical indicator for determining flood hazard intensity.

The disaster-predisposing environment refers to the external context that facilitates disaster occurrence, while the sensitivity of the disaster-predisposing environment reflects the extent to which these environmental conditions respond to and accelerate the initiation and evolution of disasters [33]、[34]. In the piedmont plain of the Taihang Mountains, topographic factors including elevation and slope regulate the flow velocity of water through drainage networks and catchments. The region is characterized by a dense network of water systems: river network density serves as an indicator of hydrological system development, with higher density corresponding to enhanced channel incision, concentrated runoff, and accelerated confluence. Additionally, distance to rivers determines the degree of flood exposure—areas in proximity to rivers are subject to the most severe flood impacts, making this factor critical for identifying flood-vulnerable zones [35]. Accordingly, this study selects elevation, slope, river network density, and distance to water bodies as the core indicators for evaluating the sensitivity of the disaster-predisposing environment.

The vulnerability of disaster-bearing bodies refers to the degree of loss incurred by humans and their social resources when exposed to disasters [36]、[37]. In this study, three indicators are selected: population density, GDP per unit area, and the proportion of the primary industry. Higher population density and GDP per unit area increase the susceptibility to adverse impacts during disaster events. The proportion of the primary industry reflects both the sensitivity to hydroclimatic conditions and the resilience to recovery of the region.

Disaster prevention and mitigation capacity (R) refers to the adaptive measures implemented to mitigate the impacts of flood disasters [22]、[38]. For the dimension of disaster prevention and mitigation capacity, common evaluation indicators include the number of hospital beds, flood control standards, and drainage standards. Higher values of these indicators signify enhanced social development and improved protective capabilities, which can reduce flood vulnerability to a certain extent. In this study, medical service capacity and emergency expenditure capacity are selected as the core evaluation indicators.

Table I Flood Disaster Risk Assessment Indicator System for the Alluvial-Diluvial Plain in the Piedmont of the Taihang Mountains

Target layer	Principle layer	Index leve	Indicator Impact	Data source
Risk Assessment of Flood Disasters	Hazard of Disaster-Causing Factors	Maximum intensity of Heavy Rainfall	+	China Meteorological Data Network
		Average rainfall	+	China Meteorological Data Network
		Peak flood discharge	+	China Meteorological Data Network
	Sensitivity of Disaster-Prone Environment	Digital Elevation Model	-	Geospatial Data Cloud
		Slope	-	Geospatial Data Cloud
		River network density	-	Geospatial Data Cloud
		Water System Distance	+	Geospatial Data Cloud
	Vulnerability of Disaster-Bearing Bodies	Gross Domestic Product	+	NASA's Goddard Space Flight Center
		Population Density	+	county/district government websites
		Proportion of the primary industry	+	county/district government websites
	Disaster Prevention and Mitigation Capability	Medical Capacity	-	county/district government websites
		Expenditure for Emergency Management	-	county/district government websites

2) Determination of Weights for the Evaluation Factor System: Determination of Subjective Indicator Weights via the Analytic Hierarchy Process (AHP). The AHP, a systematic analysis and decision-making method proposed by Saaty in the 1970s, decomposes complex decision problems into hierarchical structures. It constructs pairwise comparison judgment matrices to derive the relative weights of individual indicators. By effectively integrating expert experience and qualitative judgments, AHP has been widely applied in domains such as flood risk assessment, with its core steps encompassing judgment matrix construction, weight calculation, and consistency testing [3]、[39]、[40]. Given the method's extensive prevalence in existing literature, the specific calculation formulas for factor weights are not elaborated herein.

Objective Weight Determination of Indicators via the CRITIC Method. The CRITIC method, an objective weighting approach proposed by Diakoulaki et al. (1995), is capable of identifying and downweighting information-redundant indicators, thereby rendering the weight allocation more scientific and rational (Equation (1-7)) [41].

(1) Standardization processing

(1) This study adopts the Min-Max normalization method to standardize raw data, thereby eliminating the influence of dimensionality. For positive indicators (higher values indicate greater risk), refer to Equation (1); for negative indicators (lower values indicate greater risk), refer to Equation (2):

$$x'_{ij} = (x_{ij} - minX)/(maxX - minX) \tag{1}$$

$$x'_{ij} = (maxX - x_{ij})/(maxX - minX) \tag{2}$$

(2) Calculate indicator variability

(2) Variability is quantified by the standard deviation S of the indicator, which reflects the degree of variation in the j-th indicator across samples. A larger standard deviation indicates a higher information content:

$$\overline{x}_j = \frac{1}{n}\sum x_{ij} \tag{3}$$

$$S_j = \sqrt{\frac{\sum_{i=1}^{n}\left(x_{ij} - \overline{x}_j\right)^2}{n-1}} \tag{4}$$

(3) where $\overline{x}_j$ is the standardized mean of the *j*-th indicator.

(3) Calculation of indicator conflict

(4) Conflict reflects the degree of information independence between the *j*-th indicator and other indicators. The Pearson correlation coefficient r_{ij} is employed to measure the linear correlation between indicator *i* and indicator *j*.

$$R_j = \sum_{i=1}^{n}\left(1 - r_{ij}\right) \tag{5}$$

(4) Calculation of indicator information volume

(5) The information content C_j comprehensively accounts for both the variability of the indicator itself and its degree of independence from other indicators. A higher value of C_j indicates a greater information contribution of the indicator to the evaluation system.

$$C_j = S_j \times R_j \tag{6}$$

(5) Determine objective weights

(6) The information content of each indicator is normalized to derive the CRITIC objective weight vector W_j.

$$W_j = {C_j}\Big/{\sum_{i=1}^{n} C_j} \tag{7}$$

Determination of Comprehensive Indicator Weights Based on the Game-Theoretic Combinatorial Weighting Method. The game-theoretic combinatorial weighting method is designed to optimize the objective function under the influence of multiple factors. By integrating the results of the AHP subjective weighting method and the CRITIC objective weighting method, the optimal weights are derived [3].

(1) Calculate the initial weights

To fully leverage the respective advantages of subjective and objective weighting methods, the initial weights are determined by a linear combination of the weights obtained from the Analytic Hierarchy Process (AHP), denoted as $w^{(1)}$, and those derived from the CRITIC method, denoted as $w^{(2)}$ (Equation (8)). Here, α_1 and α_2 are combination coefficients representing the relative contributions of the two weighting results.

$$W = \alpha_1 w^{(1)} + \alpha_2 w^{(2)} \tag{8}$$

where $\alpha_1 + \alpha_2 = 1$, $\alpha_k \geq 0$

(2) Optimization objective

The formulation is given by Equation (9) below.

$$min \sum_{k=1}^{2} \parallel W - w^{(k)} \parallel_2^2 \tag{9}$$

(3) Compute the partial derivatives of the function with respect to α_1 and α_2, and set them to zero to derive the system of linear equations.

$$\begin{bmatrix} w^{(1)} \cdot w^{(1)} & w^{(1)} \cdot w^{(2)} \\ w^{(2)} \cdot w^{(1)} & w^{(2)} \cdot w^{(2)} \end{bmatrix}\begin{bmatrix} \alpha_1 \\ \alpha_2 \end{bmatrix} = \begin{bmatrix} w^{(1)} \cdot w^{(1)} \\ w^{(2)} \cdot w^{(2)} \end{bmatrix} \tag{10}$$

where $\mathrm{w}^{(k)} \cdot \mathrm{w}^{(l)} = \sum_{i=1}^{n} \mathrm{w}^{(k)}{}_i \cdot \mathrm{w}_i^{(l)}$ is the dot product of vectors, *n* is the number of evaluation indicators.

(4) Normalized Combination Coefficients.

$$\alpha_k^* = \frac{|\alpha_k|}{\sum_{j=1}^{2}|\alpha_j|} \tag{11}$$

(5) Final combined weights.

$$w^* = \alpha_1^* w^{(1)} + \alpha_2^* w^{(2)} \quad (12)$$

3) Flood Disaster Risk Assessment Model: Flood risk is a comprehensive assessment of potential losses and damages from flooding, establishing a four-dimensional risk evaluation framework of H–E–V–R, whose conceptual description can be expressed as [42].

$$R = \sum_{j=1}^{n} w_j^* x_{ij} \quad (13)$$

In the formula, R represents flood disaster risk, which is jointly determined by hazard factor danger level, disaster-prone environmental sensitivity, vulnerability of exposed elements, and disaster prevention and mitigation capacity; x_{ij} denotes the value of each indicator, and w_j^* represents the weight of each indicator.

III. RESULTS

A. Weight

Weight results derived from different weighting methods exhibit discrepancies. The weights obtained via the game-theoretic combinatorial weighting approach integrating AHP (Equation (1–7)) and CRITIC (Equation (8–13)) are presented in Table II. All evaluation matrices in the AHP method passed the consistency test.

Within the Analytic Hierarchy Process (AHP) framework, the top five weighted factors are distance from water systems (0.2440), rainfall intensity (0.1496), population density (0.1001), and elevation-slope (0.0934), whereas river network density (0.0365), medical capacity (0.0318), and the proportion of primary industry (0.0219) exhibit the lowest weights. This method reveals that flood disasters in the alluvial-proluvial plain area at the piedmont of the Taihang Mountains are primarily governed by proximity to rivers—with flood susceptibility increasing as distance to rivers decreases. Furthermore, flood occurrences are also significantly influenced by rainfall intensity, population density, and terrain conditions.

Objective weights for standardized indicators were computed using the CRITIC method, yielding rankings that exhibit certain discrepancies from the subjective weights derived via AHP. Among the CRITIC-derived objective weights, distance to water systems (0.1935) ranks the highest, followed by peak flood discharge (0.1521) and the proportion of primary industry (0.1391). Notably, population density—previously a top-ranked factor in the subjective weight system—has a markedly lower objective weight (0.0249). This discrepancy arises from the CRITIC method's inherent preference for indicators with high spatial variability and low information redundancy: distance to water systems and peak flood discharge demonstrate distinct spatial gradients and high independent information content, whereas population density exhibits relatively homogeneous spatial distribution across the study area, resulting in its lower objective weight. Population density (0.0249), emergency investment (0.0176), and GDP (0.0173) are assigned the smallest weights in the CRITIC framework.

The game-theoretic composite weights reveal that distance to water systems (0.2220), rainfall intensity (0.1370), and peak flood discharge (0.1127) are the top contributors to flood risk. Among the four evaluation dimensions, the hazard (H) dimension accounts for the largest share (31.05%), with rainfall intensity and peak flood discharge jointly contributing nearly one-quarter of this proportion. The sensitivity dimension (54.74%) is dominated by distance to water systems (22.20%), which was assigned high weights by both the AHP and CRITIC methods—reflecting its consistent importance across subjective and objective frameworks, hence receiving a higher composite weight. The vulnerability dimension (16.94%) is characterized by the dominance of the primary industry proportion, while the combined weight of population and economic indicators is less than 10%. For the disaster prevention and mitigation capacity dimension (8.53%), the weights of Medical Capacity and Expenditure for Emergency Management show significant discrepancies between the AHP and CRITIC results; however, the game-theoretic combination yields more converged weight outcomes.

TableII Game theory combination weights

Index	AHP Weights	CRITIC Weights	Game theory combination weights
Maximum intensity of Heavy Rainfall	0.1496	0.1207	0.1370
Average rainfall	0.0453	0.081	0.0608
Peak flood discharge	0.0823	0.1521	0.1127
Digital Elevation Model	0.0934	0.0608	0.0792
Slope	0.0934	0.0386	0.0695
River network density	0.0365	0.0995	0.0640
Water System Distance	0.2440	0.1935	0.2220
Gross Domestic Product	0.0382	0.0173	0.0291
Population Density	0.1001	0.0249	0.0673
Proportion of the primary industry	0.0219	0.1391	0.0730
Medical Capacity	0.0318	0.0548	0.0418
Expenditure for Emergency Management	0.0636	0.0176	0.0435

B. Flood Disaster Risk Assessment Results

Based on the weights obtained through combined weighting and formula (13), the results for each dimension

(Fig. 2) and the comprehensive risk assessment results (Fig. 3a) are derived.

The hazard intensity of disaster-causing factors exhibits significant spatial heterogeneity, presenting an overall west-to-east decreasing gradient pattern (Fig. 2a). High-hazard areas account for 3.54% of the total study area, primarily concentrated in the alluvial-proluvial plain zone at the piedmont of the Taihang Mountains in the west, extending as continuous linear belts along the mountain range orientation. Moderately high-hazard areas occupy 9.60% of the area, characterized by patchy spatial patterns—predominantly distributed around urban agglomerations such as Beijing, Shijiazhuang, and Hebi in the west, with a few scattered patches in the east. Moderate-hazard areas cover 27.92% of the area, forming discontinuous linear belts stretching from the northeast to the central-west and southeast, showing a spatial coupling relationship with regional topographic transition zones and major water system corridors. Moderately low-hazard areas make up 28.22%, concentrated along the Southern Canal in the east and the Tang River basin in the northwest. Low-hazard areas account for 30.73%, appearing as isolated block-like structures, mainly located in the relatively flat inland plains of the central-southern and central-northern regions.

The sensitivity of the disaster-pregnant environment exhibits significant spatial agglomeration characteristics, with high-value areas primarily concentrated along major river systems, forming an overall radial decreasing distribution pattern extending from the Bohai Bay to inland rivers in the west (Fig. 2b). High-sensitivity and moderately high-sensitivity areas together account for 42.40% of the total study area, which are highly clustered in typical flood-prone regions with dense hazard-bearing bodies—including the Yongding River floodplain in the northeast, the Dongdian flood storage and detention area in the central-south, and the Dazhuze–Ningjinbo flood storage and detention area. Moderate and moderately low-sensitivity areas are distributed in zonal or banded patterns surrounding the periphery of high- to moderately high-sensitivity areas, accounting for 32.92% of the total area; low-sensitivity areas are scattered in patchy formations, concentrated in the outer areas of river systems, with the two types of areas collectively accounting for 24.69%.

The vulnerability of hazard-bearing bodies exhibits an overall spatial differentiation pattern with higher values in the central region and lower values in the northern and southern regions (Fig. 2c). High-vulnerability and moderately high-vulnerability areas account for 43.78% of the total study area, primarily distributed as continuous block-shaped clusters in the central alluvial-proluvial plain at the piedmont of the Taihang Mountains, with a few scattered patchy distributions in the northern region. These areas are highly spatially coupled with core hazard-bearing body agglomerations characterized by high population density and large GDP aggregates. Moderate-vulnerability areas occupy 22.38% of the area, mainly concentrated in the central plain hinterland and showing a block-like spatial distribution. Low-vulnerability and moderately low-vulnerability areas together account for 33.84%, distributed in patchy patterns and primarily concentrated in the southwestern piedmont zone of the Taihang Mountains and the northeastern downstream plain of the Haihe River Basin.

Spatially, the disaster prevention and mitigation capacity presents an overall differentiation pattern of "low in the central area and high in the surrounding areas" (Fig. 2d). Low-value and moderately low-value areas jointly account for 4.99% of the total study area, which are highly concentrated in the built-up areas of core cities such as Beijing, Tianjin, and Shijiazhuang—indicating that these regions have relatively high levels of medical resource allocation and emergency fiscal expenditure intensity, and thus their comprehensive disaster prevention and mitigation capacity is actually relatively strong. Moderately high-value areas are mainly distributed in the peripheral counties of the study area, showing a scattered block-like pattern, with their capacity levels generally falling in the lower-middle range. This reflects that there is still a significant spatial imbalance in regional disaster prevention and mitigation capacity building, and there is an urgent need for systematic improvement in the peripheral areas.

The risk assessment results exhibit an overall spatial differentiation pattern of "high in the northern, central, and southern regions, and low in the surrounding areas" (Fig. 3a). By risk level classification: high-risk areas account for 15.03%, moderately high-risk areas for 27.07%, moderate-risk areas for 20.53%, moderately low-risk areas for 20.03%, and low-risk areas for 17.35%. The spatial distribution characteristics are as follows: High-risk areas extend in a zonal pattern along major river systems such as the Yongding River, Hutuo River, and Zhangwei River, concentrating in core urban agglomerations in the northern region (Beijing, Tianjin, Langfang), central region (Shijiazhuang), and southern region (Xinxiang). Moderately high-risk areas generally inherit the spatial orientation of high-risk areas, primarily distributed in the mid-northern Ziya River Basin and mid-southern Fuyang River Basin. Moderate-risk areas are mainly clustered in the peripheral zones of high- and moderately high-risk areas, showing a zonal distribution. Low-risk and moderately low-risk areas are scattered in patchy formations, mostly located in the central plain hinterland far from the main river systems.

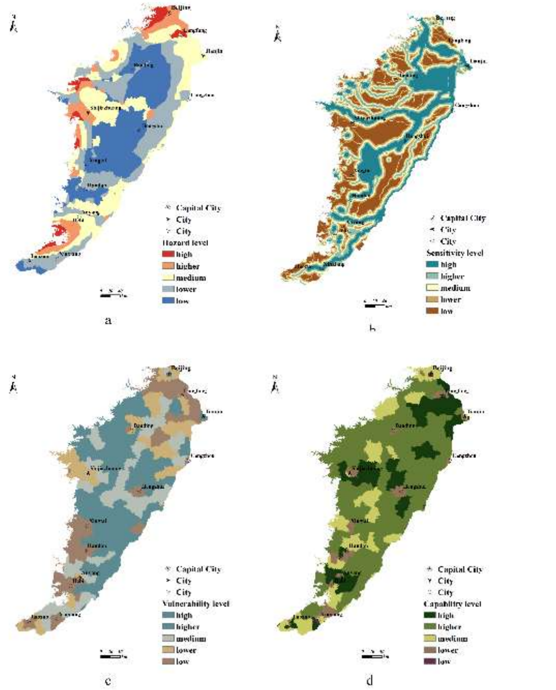

Fig. 2 Distribution of flood risk dimensions: (a) H, (b) S, (c)V, (d) R

IV. Discussion

A. *Reliability of Results*

To verify the reliability of the risk assessment results, a spatial overlay analysis was performed using county-level historical flood inundation frequency data spanning 2000–2022 [43]. The results indicate that 70.59% of the identified high-risk and very-high-risk areas overlap with regions where the historical inundation frequency is ≥ 3 times, revealing a strong spatial coupling relationship between high-risk zones and historically flood-prone areas. This finding demonstrates that the assessment results effectively capture the cumulative effects of historical disaster-causing processes. Flood risk is a comprehensive outcome of the combined effects of hazard, sensitivity, vulnerability, and disaster prevention and mitigation capacity, whereas historical inundation frequency only characterizes the hazard dimension—thus, the two are not fully consistent. However, the 70.59% overlap rate at the county scale provides empirical support for the reasonableness of the assessment results.

Furthermore, this study further adopted the extreme scenario characterized by the 100-year return period flood inundation extent to conduct spatial consistency validation for high-hazard and very-high-hazard zones (Fig. 2b). The results indicate that 73.97% of high-hazard and very-high-hazard units are located within the inundation extent with a depth greater than 0.5 m, demonstrating that the assessment results effectively depict the spatial pattern of potential hazards under extreme flood events. The integrated hazard assessment, which comprehensively considers multiple factors including hazard agent risk, disaster-forming environment sensitivity, and disaster prevention and mitigation capacity, further verifies the robustness and applicability of the assessment system.

Thus, the validation from two dimensions—historical disaster frequency and extreme scenario inundation extent—demonstrates that the risk assessment results exhibit sound reasonableness and high credibility.

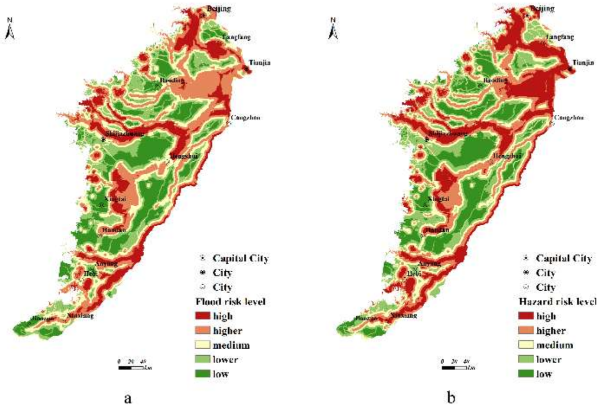

Fig. 3 Assessment Results of Flood Disaster Risk and Hazard in the Study Area: (a) Flood Disaster Risk, (b) Flood Disaster HazardFlood disaster risk distribution maps

B. *Key Influencing Factors and Strategic Recommendations for the Spatial Distribution of Flood Disaster Risk in the Piedmont Area of the Taihang Mountains*

Flood disaster assessment necessitates an understanding of its causal mechanisms. Historical flood impact records indicate a general increase in flood-induced impacts, which is primarily driven by economic expansion and population growth [44]. The assessment results reveal a spatial pattern of the Taihang Piedmont area characterized by high flood risk in the northern, central, and southern segments, with low risk in the peripheral regions. High-risk zones are predominantly concentrated in core urban centers including Beijing, Shijiazhuang, and Xinxiang, and are distributed along the Yongding River, Hutuo River, and Zhangwei River systems; low-risk areas are mainly located in the Xingtai area. This spatial pattern is highly consistent with the rainfall characteristics, river system distribution, topographic conditions, and the agglomeration of socioeconomic activity factors in the Taihang Piedmont area.

From the perspective of natural factors, the occurrence probability of regional flood disasters is jointly determined by hazard agents and disaster-forming environments. Results of game theory-based weighting show that the weights of distance to water systems, rainfall intensity, and peak flood discharge account for the largest proportion, totaling nearly 50%. In the Taihang Piedmont Plain, rainfall processes and water system distribution serve as the dominant factors shaping the spatial heterogeneity of regional flood risk.

Additionally, elevation contributes 7.92% to the combined weight, ranking fourth—this further indicates that topographic conditions elevate the probability of flood disasters. Given the "high in the northern, central, and southern segments, low in the periphery" risk spatial pattern derived from regional rainfall, topography, and other influencing factors, it is imperative to strengthen hydrometeorological monitoring and early warning systems, restrict the intensity of local engineering development, and prioritize engineering governance and risk-avoidance relocation. In line with the flood control strategy of "upstream storage, midstream drainage, downstream discharge, and effective flood management," efforts should focus on reinforcing embankments and dredging drainage channels of dams and regional rivers to enhance flood conveyance capacity; implementing zonal management of flood storage and detention areas to retain their regulation and isolation functions; and improving safety facilities and compensation mechanisms.

Flood disaster risk is also shaped by socioeconomic activities. Integrated weighting results reveal that low-risk areas are characterized not only by low precipitation and sparse river networks, but also by small population size, low economic development level, and low vulnerability of disaster-bearing bodies. In contrast, high-risk core urban centers such as Beijing and Tianjin show that high population density and medical capacity exert significant impacts on flood occurrence. Disaster risk management necessitates the integrated implementation of engineering and non-engineering measures, which aim to reduce the hazard intensity of hazard agents, minimize the exposure of disaster-bearing bodies, enhance the resilience of disaster-affected systems, and comprehensively improve regional disaster prevention and mitigation capacities. Specifically, efforts may focus on promoting regular physical exercise among the public, advancing national fitness initiatives, and strengthening emergency response and post-disaster recovery capacities at the community level.

In conclusion, high-risk areas are primarily shaped by the combined effects of dominant natural factors (i.e., rainfall, topography, and water systems) and anthropogenic conditions (including high population density, economic development level, and disaster prevention capacity). While natural conditions exert a more pronounced influence on flood disasters, effective risk governance and enhanced regional resilience can substantially mitigate potential losses.

V. CONCLUSIONS

Taking the Taihang Piedmont Plain as the research object, this study constructs a flood disaster risk assessment index system based on the disaster risk system theory, covering four dimensions: hazard agent hazard, disaster-forming environment sensitivity, disaster-bearing body vulnerability, and disaster prevention and mitigation capacity. A game-theoretic combined weighting method integrating the Analytic Hierarchy Process (AHP) and the Criteria Importance Through Inter-criteria Correlation (CRITIC) method (which accounts for inter-indicator correlations) is adopted to determine indicator weights, thereby realizing the assessment of flood disaster risk and the delineation of risk spatial distribution patterns in the study area. The main conclusions are as follows:

(1) The flood disaster risk in the Taihang Piedmont Plain exhibits significant spatial heterogeneity, characterized by a distribution pattern of higher risk in the northern, central, and southern segments and lower risk in the peripheral regions. High-risk zones are primarily concentrated along major river systems including the Yongding River, Hutuo River, and Zhangwei River, clustered in core urban agglomerations such as Beijing, Tianjin, Langfang, Shijiazhuang, and Xinxiang, and extend along these river corridors. Moderately high-risk areas are mainly distributed in the mid-northern Ziya River Basin and the mid-southern Fuyang River Basin. Low- and relatively low-risk zones are predominantly located in the central region distant from major water systems.

(2) Indicator weight analysis results reveal that distance to water systems, rainfall intensity, peak flood discharge, and elevation are the most influential factors, acting as key driving forces for flood disaster risk formation in the study area. Among these, distance to water systems reflects the spatial pattern of flood flow direction and its outward diffusion process; high rainfall intensity and peak flood discharge represent the fundamental hydrological conditions underpinning regional flood occurrence; elevation further exacerbates spatial disparities in flood disaster risk between mountain passes and plain areas. Additionally, high population density, high economic development level, strong vulnerability of disaster-bearing bodies, and insufficient medical service capacity exert significant differential impacts on the spatial distribution of risk.

(3) The frequency of historical disasters and inundation extent validate the rationality of the assessment results. Among counties with a historical disaster frequency of ≥3 occurrences over the past 22 years, 70.59% correspond to high-risk zones in the assessment; meanwhile, the spatial consistency between inundation areas and regional disaster risk assessment results reaches 73.97%. These findings indicate that the risk assessment model can effectively identify historically disaster-prone regions, demonstrating notable reliability. The assessment outcomes can provide a scientific basis for flood disaster risk management and prevention in the Taihang Piedmont Plain.

Declarations

Acknowledgments

The authors would like to convey their heartfelt gratitude to the anonymous editor and reviewers for their time and effort in reviewing and providing helpful feedback on the article.

Authors' statement

All authors have read, understood, and have complied as applicable with the statement on "Ethical responsibilities of Authors" as found in the Instructions for Authors.

Funding

This work was supported in part by the Science and Technology Innovation Program for Postgraduate Students in IDP subsidized by the Fundamental Research Funds for the Central Universities (ZY20250337)， Student Innovation Training Program Project of University of Emergency Management（202611104002）the Langfang Science and Technology Research and Development Plan Self-Funded Project of China (2025013012)，the Fundamental Research Funds for the Central Universities of CIDP(ZY20215144).

Competing Interests

The authors have no relevant financial or non-financial interests to disclose.

Data availability

The original contributions presented in the study are included in the article, further inquiries can be directed to the corresponding author.

Author contributions

Yixin Pang: Conceptualization, Formal analysis, Methodology, Visualisation, Writing – original draft, Writing – review and editing

Haijun Li: Methodology, Writing – original draft, Writing – review and editing

Ziyan Zhang: Resources, Writing – original draft, Writing – review and editing

Yao Fan: Resources, Writing – review and editing

Bingbin Du, Shuiqing Zhou,Jiachen Lu, Xiaoqing Yu:Data curation, Writing – review and editing

References

[1] E. O. Farooq, M. N. Khalil, R. S. Mahmood, and A. Jan, “Policy Research Journal FLOOD RISK ASSESSMENT AND MANAGEMENT USING HYDROLOGICAL MODELING AND GIS TECHNIQUE”, doi: 10.5281/zenodo.19675848.

[2] M. A. Mukhtar *et al.*, “Integrated flood risk assessment in Hunza-Nagar, Pakistan: unifying big climate data analytics and multi-criteria decision-making with GIS,” *Front. Environ. Sci.*, vol. 12, 2024, doi: 10.3389/fenvs.2024.1337081.

[3] G. Li, W. Shao, Y. Li, Y. Zhao, Y. Zhang, and T. Song, “Urban flood risk assessment based on the combination weight of game theory: a case study of Jinan City, China,” *Sci. Rep.*, vol. 16, no. 1, p. 4176, Jan. 2026, doi: 10.1038/s41598-025-34309-4.

[4] Y. Li, C. He, X. Shi, and K. Hussain, “How to respond effectively to extreme flood events? Lessons from non-frequently flooded rural communities in northern China,” *Habitat Int.*, vol. 173, p. 103809, Jul. 2026, doi: 10.1016/j.habitatint.2026.103809.

[5] L. Ying and Z. Shan-Shan, “Floods losses and hazards in China from 2001 to 2020,” *Li Y, Zhao S S.*, vol. 18, pp. 154–165, Mar. 2022.

[6] ZHANG Jing, XU Hongmei, HAO Lisheng, LIU Lüliu, and XIANG Liang, “Projected Changes in Extreme Precipitation over Haihe River Basin Based on a Variable-Resolution Community Earth System Model,” *Climatic and Environmental Research*, vol. 30, pp. 373–386, 2025.

[7] L. HAO, L. HE, S. CHENG, and S. LIANG, “Climatic characteristics and monitoring analysis of rainy season in the Haihe River Basin,” *Progress in Geography*, vol. 40, no. 7, pp. 1181–1194, 2021, doi: 10.18306/dlkxjz.2021.07.009.

[8] Ruihua Li, Ting Huang, and Chao Wang, “Comprehensive Ecological Environment Quality Assessment Based on AHP and CRITIC Weight Method—Taking Turpan and Hami Cities as Examples,” *Adv. Appl. Math.*, vol. 13, no. 07, pp. 3341–3355, 2024, doi: 10.12677/aam.2024.137320.

[9] LI Xiucang, LI Wei, ZHOU Xingyan, HONG Haixu, GAO Hui, and SUN Linhai, “Analysis ofthe rainfall background and implications of the ‘25·7’ regional major flood in the Haihe River Basin,” *China Flood & Drought Management*, vol. 35, pp. 1–5, Nov. 2025.

[10] J. Xie, Y. He, and X. Chen, “Disaster loss-based flood risk assessment of the Guangdong-Hong Kong-Macao Greater Bay Area and the differentiated spatial pattern,” *J. Clean. Prod.*, vol. 561, May 2026, doi: 10.1016/j.jclepro.2026.148418.

[11] J. W. Hall, R. J. Dawson, P. B. Sayers, C. Rosu, J. B. Chatterton, and R. Deakin, “A methodology for national-scale flood risk assessment,” *Proceedings of the Institution of Civil Engineers - Water and Maritime Engineering*, vol. 156, no. 3, pp. 235–247, Sep. 2003, doi: 10.1680/wame.2003.156.3.235.

[12] Ö. Ekmekcioğlu, K. Koc, and M. Özger, “District based flood risk assessment in Istanbul using fuzzy analytical hierarchy process,” *Stochastic Environmental Research and Risk Assessment*, vol. 35, no. 3, pp. 617–637, Mar. 2021, doi: 10.1007/s00477-020-01924-8.

[13] N. Tabasi, M. Fereshtehpour, and B. Roghani, “A review of flood risk assessment frameworks and the development of hierarchical

structures for risk components," *Discov. Water*, vol. 5, no. 1, p. 10, 2025, doi: 10.1007/s43832-025-00193-2.

[14] C. Wei-shuai, C. Jin, and L. Dan, "Review on flood risk assessment," *Journal of Yangtze River Scientific Research Institute*, vol. 27, pp. 18–24, Sep. 2010.

[15] G. Huang *et al.*, "Study on risk analysis and zoning method of urban flood disaster," *Water Resour Prot*, vol. 36, pp. 1–6, 2020, doi: 10.3880/j.issn.1004-6933.2020.06.001.

[16] C. E. Amatebelle, S. T. Owolabi, A. A. Ogundeji, and C. C. Okolie, "A systematic analysis of remote sensing and geographic information system applications for flood disaster risk management," *J Spat Sci*, vol. 70, no. 3, pp. 441–467, Jul. 2025, doi: 10.1080/14498596.2025.2476973.

[17] Z. Xu, X. Lu, and Q. Shi, "Research progress on urban flooding disaster characteristics and risk assessment," *Adv. Sci. Technol. Water Resour.*, vol. 45, pp. 1–9, 46, 2025, doi: 10.3880/j.issn.10067647.2025.01.001.

[18] LI Chaochao, TIAN Juncang and SHEN Ruozhu, and SHEN Ruozhu, "Review on Assessment of Flood and Waterlogging Risk," *Journal of Catastrophology*, vol. 35, pp. 131–136, 2020, doi: 10.3969/j.issn.1000-811X.2020.03.025.

[19] G. Li, J. Liu, and W. Shao, "Research progress in flood disaster risk assessment and zoning," *J. China Hydrol.*, vol. 43, pp. 15–20, Aug. 2023, doi: 10.19797/j.cnki.1000-0852.20220157.

[20] R. Sharker *et al.*, "GIS-based AHP approach to flood susceptibility assessment in Tangail district, Bangladesh," *J. Earth Syst. Sci.*, vol. 134, no. 1, p. 26, Jan. 2025, doi: 10.1007/s12040-024-02480-3.

[21] G. Zhu, S. Fang, C. Yin, F. Yu, and X. Qi, "Risk assessment of rainstorm-flood disaster based on FAHP-CRITIC: Taking Lintong District of Xi'an City as an example," *Water Resour. Hydropower Eng.*, vol. 54, pp. 37–48, 2023, doi: 10.13928/j.cnki.wrahe.2023.04.003.

[22] C. Li *et al.*, "Review on Urban Flood Risk Assessment," Jan. 01, 2023, *MDPI*. doi: 10.3390/su15010765.

[23] Y. J. Chen, H. J. Lin, J. J. Liou, C. T. Cheng, and Y. M. Chen, "Assessment of Flood Risk Map under Climate Change RCP8.5 Scenarios in Taiwan," *Water (Switzerland)*, vol. 14, no. 2, Jan. 2022, doi: 10.3390/w14020207.

[24] L. Bin, K. Xu, H. Pan, Y. Zhuang, and R. Shen, "Urban flood risk assessment characterizing the relationship among hazard, exposure, and vulnerability," *Environmental Science and Pollution Research*, vol. 30, no. 36, pp. 86463–86477, Aug. 2023, doi: 10.1007/s11356-023-28578-7.

[25] T. Zhang, K. Wu, X. Wang, X. Li, L. Li, and L. Chen, "Impact of Land Use Patterns on Flood Risk in the Chang-Zhu-Tan Urban Agglomeration, China," *Remote Sens. (Basel).*, vol. 17, no. 16, Aug. 2025, doi: 10.3390/rs17162889.

[26] Haiyan Wang and Zhiyan Du, "Evaluation of Site Selection Decision Based on Pythagorean Fuzzy Cloud," *Adv. Appl. Math.*, vol. 13, no. 02, pp. 672–683, 2024, doi: 10.12677/AAM.2024.132065.

[27] S. Zhou *et al.*, "Flood Disaster Risk Assessment of the Beijing-Tianjin-Hebei Region Based on Variable Fuzzy Recognition and Combined Weighting," *International Journal of Scientific Research and Engineering Development*, vol. 9, pp. 751–762, 2026, [Online]. Available: www.ijsred.com

[28] R. Xia and D.-L. Zhang, "An Observational Analysis of Three Extreme Rainfall Episodes of 19–20 July 2016 along the Taihang Mountains in North China," *Mon. Weather Rev.*, vol. 147, no. 11, pp. 4199–4220, Nov. 2019, doi: 10.1175/MWR-D-18-0402.1.

[29] A. G. Blum, P. J. Ferraro, S. A. Archfield, and K. R. Ryberg, "Causal Effect of Impervious Cover on Annual Flood Magnitude for the United States," *Geophys Res Lett*, vol. 47, no. 5, p. e2019GL086480, Mar. 2020, doi: 10.1029/2019GL086480.

[30] W. D. Shuster, J. Bonta, H. Thurston, E. Warnemuende, and D. R. Smith, "Impacts of impervious surface on watershed hydrology: A review," *Urban Water J.*, vol. 2, no. 4, pp. 263–275, Dec. 2005, doi: 10.1080/15730620500386529.

[31] M. Chang, K. Zhou, X. Dou, F. Su, and B. Yu, "Quantitative risk assessment of rainstorm-induced flood disaster in Piedmont plain of Pakistan," *Sci. Rep.*, vol. 15, no. 1, Dec. 2025, doi: 10.1038/s41598-024-84738-w.

[32] L. Liu, L. Zhou, T. Ao, X. Liu, and X. Shu, "Flood Hazard Analysis Based on Rainfall Fusion: A Case Study in Dazhou City, China," *Remote Sens. (Basel).*, vol. 14, no. 19, Oct. 2022, doi: 10.3390/rs14194843.

[33] GAO Cao, CHEN Xi, and ZHANG Fang-min et al, "GIS-based Ｒisk Assessment of Drought Meteorological Disasters on Wheat in Cangzhou City," *J．Anhui Agric．Sci．*, vol. 47, pp. 223–226, 2019.

[34] Yao Lv, Jinhu Wang, Jing Wang, Yuhao Wang, and Yuyao Wang5, "Study on Risk Assessment and Zoning of Drought Disaster Based

on GIS: A Case Study of Yangtze River Delta," *Operations Research and Fuzziology*, vol. 13, no. 03, pp. 2328–2338, 2023, doi: 10.12677/ORF.2023.133233.

[35] D. Rincón, U. T. Khan, and C. Armenakis, "Flood risk mapping using GIS and multi-criteria analysis: A greater toronto area case study," *Geosciences (Switzerland)*, vol. 8, no. 8, Aug. 2018, doi: 10.3390/geosciences8080275.

[36] L. Chen, J. Chen, and G. Gao, "Flood risk assessment in coastal cities: A case study of Lingang New City," *J Changjiang River Sci Res Inst*, vol. 42, pp. 84–93, 2025, doi: 10.11988/ckyyb.20240575.

[37] CAO Luo-dan and LI Jia-lin., "Integrated Risk Assessment of Flood Disaster in Zhejiang Province Based on RS and GIS," *Journal of Natural Disasters*, vol. 24, pp. 111–119, 2015.

[38] L. Cao, J. Li, L. Xu, Q. Yuan, M. Wang, and D. Huang, "reliminary Assessment of Flood Disaster Prevention and Mitigation Capacity in Ningbo," *J. Ningbo Univ. Nat. Sci. Eng. Ed.*, vol. 27, pp. 84–90, 2014.

[39] T. L. Saaty, "SOME MATHEMATICAL CONCEPTS OF THE AN AL YTIC HIERARCHY PROCESS."

[40] O. Rahmati, H. Zeinivand, and M. Besharat, "Flood hazard zoning in Yasooj region, Iran, using GIS and multi-criteria decision analysis," *Geomatics, Natural Hazards and Risk*, vol. 7, no. 3, pp. 1000–1017, May 2016, doi: 10.1080/19475705.2015.1045043.

[41] D. Diakoulaki, G. Mavrotas, and L. Papayannakis, "Determining objective weights in multiple criteria problems: The CRITIC method," *Computers Ops Res.*, vol. 22, pp. 763–770.

[42] Y. Gao *et al.*, "Evaluating Yangtze River Delta Urban Agglomeration flood risk using a hybrid method of automated machine learning and analytic hierarchy process," *Natural Hazards and Earth System Sciences*, vol. 25, no. 9, pp. 3087–3108, Sep. 2025, doi: 10.5194/nhess-25-3087-2025.

[43] S. Fu, D. M. Schultz, H. Lyu, Z. Zheng, and C. Zhang, "Creating a national urban flood dataset for China from news texts (2000-2022) at the county level," *Hydrol. Earth Syst. Sci.*, vol. 29, no. 3, pp. 767–783, Feb. 2025, doi: 10.5194/hess-29-767-2025.

[44] B. Merz *et al.*, "Causes, impacts and patterns of disastrous river floods," *Nat. Rev. Earth Environ.*, vol. 2, no. 9, pp. 592–609, Aug. 2021, doi: 10.1038/s43017-021-00195-3.